NANO LETTERS

2008
Vol. 8, No. 9
2638-2642

Design of Light Scattering in Nanowire Materials for Photovoltaic Applications

Otto L. Muskens,*,† Jaime Gómez Rivas,†,‡ Rienk E. Algra,‡,§,∥ Erik P. A. M. Bakkers,‡ and Ad Lagendijk†

Center for Nanophotonics, FOM Institute for Atomic and Molecular Physics AMOLF, Kruislaan 407, 1098 SJ Amsterdam, The Netherlands, Philips Research Laboratories, High Tech Campus 4, 5656 AE Eindhoven, The Netherlands, Materials Innovation Institute, 2628CD Delft, The Netherlands, and Institute for Molecules and Materials, Solid State Chemistry Department, Radboud University Nijmegen, Toernooiveld 1, 6525ED Nijmegen, The Netherlands

Received March 20, 2008; Revised Manuscript Received June 27, 2008

ABSTRACT

We experimentally investigate the optical properties of layers of InP, Si, and GaP nanowires, relevant for applications in solar cells. The nanowires are strongly photonic, resulting in a significant coupling mismatch with incident light due to multiple scattering. We identify a design principle for the effective suppression of reflective losses, based on the ratio of the nondiffusive absorption and diffusive scattering lengths. Using this principle, we demonstrate successful suppression of the hemispherical diffuse reflectance of InP nanowires to below that of the corresponding transparent effective medium. The design of light scattering in nanowire materials is of large importance for optimization of the external efficiency of nanowire-based photovoltaic devices.

Semiconductor nanowires are studied intensively for their potential use in next-generation nanoelectronic, photonic, and photovoltaic devices. Recently, there has been progress toward realization of efficient solar cells employing inorganic nanowires.[1−7] Next to the use of nanowires for electrical charge transport in dye-sensitized cells,[1,2] the functionality of semiconductor nanowires as an active layer[3−7] holds promise for novel all-inorganic photovoltaic designs. For specific designs, such as those incorporating a core−shell junction, the geometry of nanowires may be electrically superior compared with that of thin films.[4,8] It is still an open question whether nanowires hold merit from the point of view of their optical properties. Effective-medium models predict a significant reduction of the reflectance of nanowire layers due to the low effective refractive index of a composite medium consisting of nanowires suspended in air.[9] This phenomenon has been employed recently in the design of extremely absorbing carbon nanotube coatings.[10] However, nanowires fabricated from high-refractive index semiconductors like silicon (refractive index $n \simeq 3.5$) are strongly photonic even at small diameters in the nanometer range. It is therefore of importance to include light scattering in the design of nanowire photovoltaic devices.

Here, we show experimentally that, for typical wire diameters around 50 nm, the optical properties of nanowire layers are largely determined by diffuse multiple scattering of light. We find that the reflectance of such a layer can both be increased or be suppressed compared with that of a transparent effective medium, depending critically on the ratio between the absorption and the scattering mean free paths. In the case of Si nanowires, diffuse reflectance of light will be an important factor in the external efficiency for the technologically relevant diameters and volume fractions under study.[5−7] Light scattering has been employed to improve the efficiency of dye-sensitized TiO_2 solar cells in the form of dedicated scattering layers; however, attempts to control and use scattering in the active region have remained limited.[11] Surface scattering by nanoparticles has been used recently to optimize coupling of light into high-refractive index solar cells.[12,13] As we will show, volume scattering in the active layer can be employed to improve optical absorption, without the penalty of increased reflectivity, whenever the scattering mean free path can be tuned to the material absorption length.

Semiconductor nanowires of groups IV and III−V were synthesized in a low pressure (50 mbar) Aixtron 200 MOVPE reactor on native substrates of GaP(111)B, InP(111)B, and Si(111). The GaP substrate was coated with a 500 nm thick protective SiO_2 layer on the GaP(111)A side to prevent rough etching of this surface during the sample preparation.

* Corresponding author. E-mail: muskens@amolf.nl.
† FOM Institute for Atomic and Molecular Physics AMOLF.
‡ Philips Research Laboratories.
§ Materials Innovation Institute.
∥ Radboud University Nijmegen.

10.1021/nl0808076 CCC: $40.75
Published on Web 08/14/2008

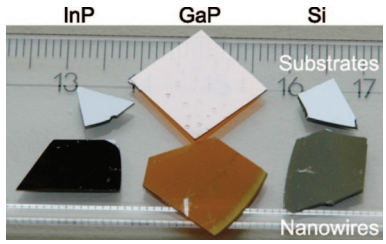

Figure 1. Photographic image of the InP, GaP, and Si nanowire materials under study (bottom row), together with their native substrates (top row).

The GaP(111)B side was etched for 2 min. with a solution of HNO_3:HCl:H_2O (2:3:3) at 80 °C, the InP(111)B was treated with a H_2SO_4:H_2O_2:H_2O (5:1:1) etch for 1 min. at room temperature, and the Si(111) substrates were etched using a standard buffered oxide etch (BOE) for 5 min. at room temperature to ensure complete removal of the surface oxides. After etching, the substrates were coated with an Au layer (30 Å for InP and Si, 3 Å for GaP) which provides a high density of nucleation centers for nanowire growth. The nanowires were grown in the VLS growth mode using trimethylindium (TMIn), trimethylgallium (TMGa), and phospine (PH_3) as precursors for InP and GaP, respectively. Disilane (Si_2H_6) was used for silicon nanowires. Growth was initiated when a temperature of 420 °C was reached by switching on the TMIn or TMGa, or 550 °C in the case of Si_2H_6. GaP nanowires were grown in a two-step process in which the wire diameter was tuned using lateral growth.[14,15] Figure 1 shows a photograph of the three nanowire materials. In contrast to their native substrates, the nanowire layers have a matte appearance, with a color varying from deep black for InP, to gray/green for Si, to orange/yellow for GaP nanowires. These differences in visual appearance reflect the difference in optical properties, as we will study in more detail.

Scanning electron microscopy (SEM) images of cleaved cross sections through the nanowire layers are shown in Figure 2a−c. Diameter distributions, determined from the SEM images, are shown on the right-hand side of Figure 2a−c. In general, the three layers show similarities in the total length, the alignment, and the average sizes of the nanowires. Some morphological differences can be observed related to the fabrication methods and to specific growth characteristics of the different materials. The InP nanowires, shown in Figure 2a, are 2.5 μm in length and very well-aligned vertically, along the crystallographic [111] direction. The wires are uniform over their length and show little tapering; only a short segment at the top is considerably thinner and can be associated to residual growth during the cooling down of the reactor. The GaP nanowires, shown in Figure 2b, have a larger diameter dispersion resulting from the coalescence of some nanowires during the lateral growth step. Higher control of VLS growth rates for the thinner wires before lateral growth results in a smoother surface layer compared with the InP wires. The Si nanowires of Figure 2c grow preferably vertically; however, repetitive twinning causes individual wires to switch growth directions along the various <111> directions. This morphology is very similar to that

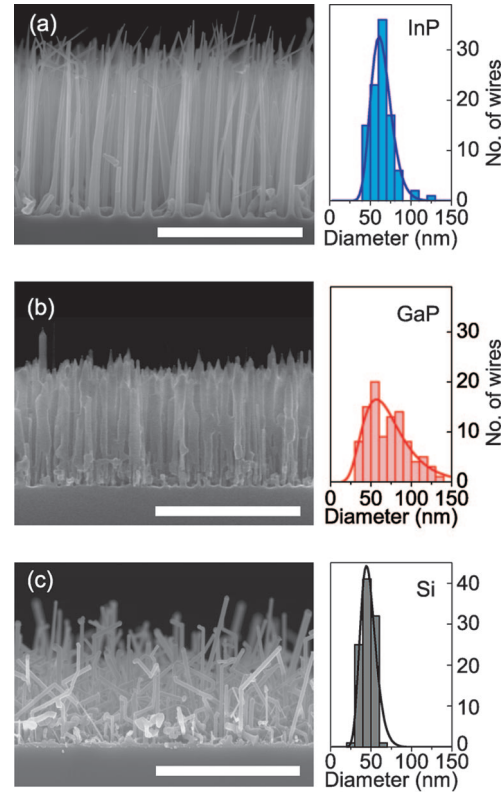

Figure 2. Cross-sectional SEM images of (a) InP, (b) GaP, and (c) Si nanowires frabricated using MOVPE growth. Scale bars represent 2 μm. (right side) Histogram of nanowire diameters of InP (blue), GaP (red), and Si (black), with lines representing log-normal fits.

of the Si nanowire layer used in solar cells.[5−7] The average (standard deviation) of the diameter distributions in Figure 2 was found to be 64(14) nm for InP, 71(24) nm for GaP, and 45(7) nm for Si nanowires.

Both specular and diffuse reflectance spectra of the nanowire layers were measured over a large spectral region from 0.7 to 2.2 eV (1650−560 nm) using a supercontinuum white-light source and visible and near-infrared fiber spectrometers. The coherent reflectance of a collimated incident light beam was determined by collecting the specularly reflected cone of light within an acceptance angle of 1°. Total reflectance spectra, including the specularly reflected beam, were measured using a gold-coated integrating sphere, allowing for measurements in the near-infrared. The diffuse reflectance was determined by subtracting the specular from the total reflectance spectra

Figure 3a−c shows the coherent (thick lines) and diffuse (thin lines) reflectance spectra of the InP (a), GaP (b), and Si (c) nanowire layers. For comparison, we show the reflectance of the bare substrates without nanowires (dashed curves in Figure 3a−c), which are in the range of 30%−40% for the materials under study. Below the electronic bandgap (1.33 eV for InP, 2.26 eV for GaP, and 1.12 eV for Si, vertical dashed lines in Figure 3), the substrates are transparent, and the backside reflection adds to the total reflectance. In the infrared, the reflectance of all of the nanowire-coated materials is strongly reduced with respect to that of the bare substrates. This reduced reflectance results from the lower

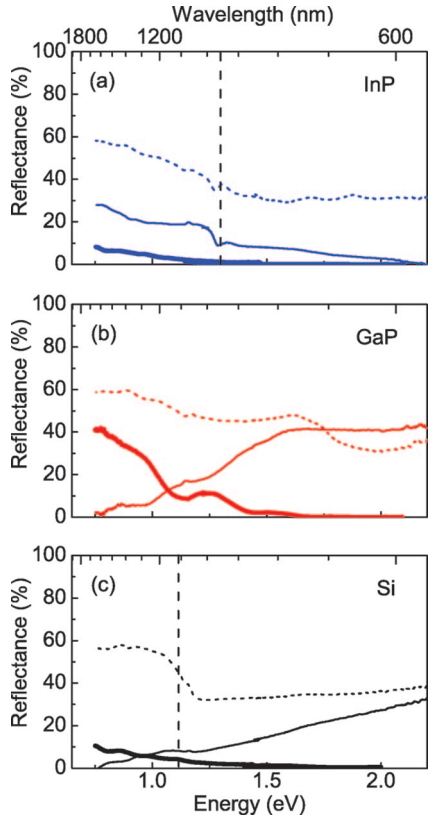

Figure 3. Experimental reflectance spectra for (a) InP, (b) GaP, and (c) Si. Lines denote the diffuse reflectance of the nanowires (thin line), the corresponding substrates (dashed line), and the coherent-beam specular reflectance (thick line). Vertical lines in (a) and (c) denote the electronic bandgaps of InP (1.33 eV) and Si (1.12 eV).

index of refraction in the nanowire artificial material, making it a stepped-index antireflection coating.[9,17] For the GaP sample, a contribution of the polished substrate backside is present in the specular reflection, while for InP and Si, the unpolished substrate does not contribute. The specular reflectance decreases strongly with increasing photon energy, reaching negligible values in the visible range above 1.5 eV.

The hemispherical diffuse reflectance for the various nanowire materials is shown by the thin lines in Figure 3a−c. For both the Si and the GaP nanowires, the diffuse reflectance is virtually absent in the infrared, while it increases strongly up to respectively 33% and 42% at 2.2 eV. This demonstrates that light scattering contributes significantly when the optical wavelength becomes shorter and comparable with the diameter of the nanowires. The small-scatterer (Rayleigh) limit[18] is valid for diameters $d \ll \lambda/(\pi n)$, which for $n = 3.5$, sets the critical diameter well below $\lambda/10$, with λ as the optical wavelength. For nanowires thicker than the critical diameter, light scattering strongly contributes to the nanowire optical properties, which for a dense collection results in diffuse transport of light. For the InP nanowires, however, the diffuse reflectance decreases strongly toward shorter wavelengths. This strikingly different behavior results from the combination of multiple scattering with strong optical absorption of InP in the visible, as will be shown below. The diffuse hemispherical reflectance of InP nanowires in the visible region drops below the specular reflectivity of an effective medium, which amounts to 2%−4% for the nanowire densities of this study.[14] This demonstrates that diffuse scattering may actually result in suppression of reflection losses compared with a transparent effective medium at the same volume fraction.

Optical characterization of the InP and Si nanowire layers was limited to reflectivity measurements due to strong light absorption in the substrates. For the GaP nanowires, grown on a double-sided polished GaP wafer, coherent-beam transmission measurements were performed. GaP is an indirect semiconductor with negligible absorption below its bandgap at 2.26 eV. Its optical properties in this spectral region are therefore determined by light scattering. From the transmission measurements, the scattering mean free path l_s was determined using the Lambert−Beer law for extinction of the coherent beam, which, in the absence of absorption, reads

$$T_{\mathrm{coh}} = e^{-l_s/L} \tag{1}$$

where L denotes the thickness of the nanowire layer. Figure 3a shows the scattering mean free path of the GaP nanowires (thin line, red). Below 1.25 eV, l_s exceeds the layer thickness and therefore could not be determined accurately. We assume that the measured scattering length of GaP nanowires will be similar to the scattering lengths of the other nanowires, since they have similar high refractive indices, wire diameters, and volume densities. We therefore compare the scattering length l_s of GaP nanowires to the absorption length, l_a, of bulk InP and Si, indicated by the respective blue and black lines in Figure 4a.[19] The absorption lengths of Si and InP differ by more than 1 order of magnitude for photon energies above 1.4 eV. For Si, l_a significantly exceeds l_s, while l_a for InP drops well below l_s above 1.33 eV. This has severe consequences on the diffuse reflectivity, as we will demonstrate using a diffusive transport model.

The diffuse optical reflectance, R_d, of a strongly scattering layer is derived from classical diffusion theory as[20]

$$R_d = \frac{\sinh\left(\frac{L-l_t}{L_a}\right) + \frac{z_2}{L_a}\cosh\left(\frac{L-l_t}{L_a}\right)}{\left(1+\frac{z_1 z_2}{L_a^2}\right)\sinh\left(\frac{L}{L_a}\right) + \frac{z_1+z_2}{L_a}\cosh\left(\frac{L}{L_a}\right)} \tag{2}$$

where l_t denotes the transport mean free path of light, which is the distance over which an incoming light beam looses all information on its original direction;[21] z_1 and z_2 are extrapolation lengths representing the effect of internal reflection at the nanowire−air and nanowire−substrate interfaces.[22,23] A diffuse absorption length L_a is introduced, defined as the characteristic distance over which the light is absorbed during diffuse transport, given by the formula[24]

$$L_a \equiv \left(\frac{1}{3} l_a l_t\right)^{1/2} \tag{3}$$

Figure 4b shows the calculated diffuse reflectance R_d for an infinitely thick layer (solid line) as well as for a thin layer with a thickness L of five mean free paths l_t (dashed line). For the calculation, we choose $z_1 = 2.0 l_t$ and $z_2 = 1.0 l_t$, corresponding to an effective refractive index of the nanowire layer[23] of around 1.4, which is a realistic estimate for the

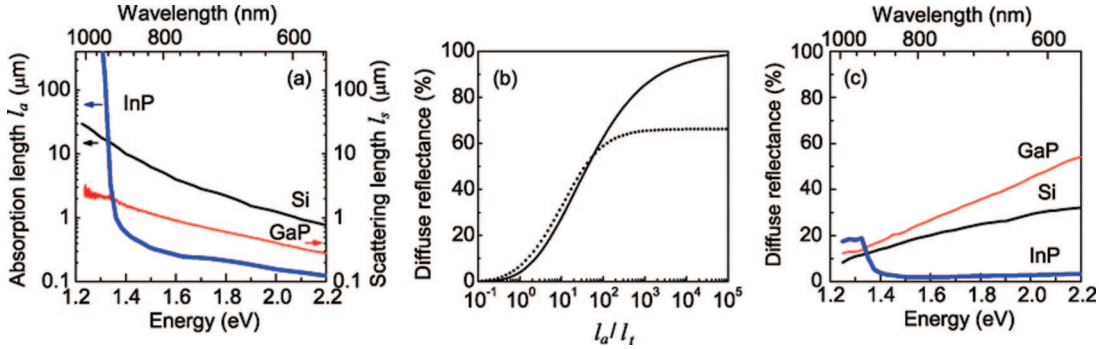

Figure 4. (a) Experimental values of the scattering length l_s of the GaP nanowires (thin line, red), together with literature values of the absorption length l_a of InP (thick line, blue) and Si (line, black), taken from ref 19. (b) Calculated diffuse reflectance R_d using eq 2 against the absorption length normalized to the mean free path l_t, for an infinite layer (solid line) and a finite layer of thickness $L = 5l_t$ (dashed line). (c) Calculated diffuse reflectance spectra of InP (thick line, blue), GaP (thin line, red), and Si (line, black) nanowires, obtained using eq 2, scattering lengths of (a), and absorption lengths corrected for nanowire volume fraction.

densities of the nanowires under study.[14] With increasing absorption length, the diffuse reflectance saturates to a value of 100% for the infinitely thick layer, while for the thin layer this value is reduced by the total transmission through the layer. The diffuse reflectance curve for the thin layer is higher than for the semi-infinite slab because of internal reflection. For a nondiffusive absorption length l_a smaller than one transport mean free path l_t, the diffuse reflectance is strongly suppressed.

By using eq 2 and the nanowire scattering and absorption lengths of Figure 4, the diffuse reflectance can be calculated as a function of energy for the three nanowire materials under study. The nondiffusive absorption length l_a of the nanowire layer was corrected for the limited volume fraction of absorbing material of around 30%. We do not consider effects of geometrical resonances on the absorption, which have been proposed as a potential means to improve the efficiency of solar cells.[6,9] For thin wires, optical absorption is actually reduced by geometrical depolarization effects.[18,25] Further, it is assumed that $l_t = l_s$, which amounts to isotropic scattering; for anisotropic scattering materials $l_t > l_s$.[21] We realize the limited validity of the isotropic scattering assumption for some of the highly aligned nanowire layers under study; however, a detailed treatment of anisotropic scattering goes beyond the scope of this Communication and would only result in an overall correction of the ratio l_t/l_a and not in a change of the observed trend.

The diffuse reflectance spectra calculated using eq 2 are shown in Figure 4c, for nanowires made of InP (blue line), GaP (red line), and Si (black line). The key observation of Figure 3, namely, the increase of the GaP and Si reflectance and the strong decrease of the InP reflectance with increasing photon energy, is reproduced quantitatively. The low diffuse reflectance of the InP nanowires means that most of the light is absorbed before it is scattered out of the layer. The effective folding up of the multiple scattering light paths inside the active nanowire layer can thus be used to enhance the absorption efficiency in nanowire solar cells. According to eq 3, the diffuse absorption length L_a will be smaller by a factor $\sqrt{3}$ than the nondiffuse material absorption length l_a in the situation that $l_s \simeq l_a$. Therefore, by properly designing the scattering properties of the nanowires, the active layer thickness of nanowire solar cells can be reduced considerably.

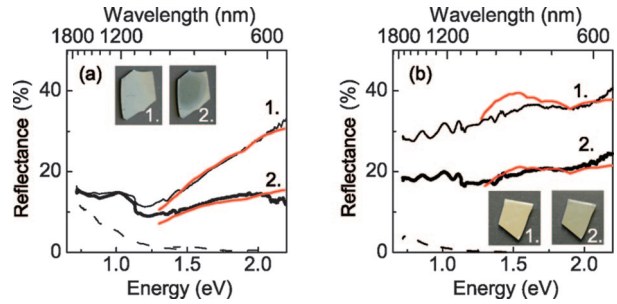

Figure 5. (a) Total hemispherical reflectance of the Si nanowire layer of Figure 2c, (1) before (thin line, black) and (2) after (thick line, black) infiltration with ethanol. Dashed line denotes specular reflectivity before infiltration. (b) Same for a layer of 30 μm long Si nanowires. Red lines in (a) and (b) are calculations using eq 2 and the optical constants of Figure 4a corrected for nanowire filling fraction, assuming an increase of l_s by a factor 3.0 after infiltration. Optical photographs of samples are shown before (1) and after (2) infiltration, using identical illumination conditions. Image scale: ~1 cm.

Conversively, the use of Si as a base material for nanowire solar cells will require the tailoring of the scattering mean free path to values larger than the absorption length, which amounts to several micrometers for the spectral region of interest. A reduction of the scattering contribution can be achieved by filling up the voids between nanowires with a higher-index medium. By using standard index matching media, a three-fold increase of the scattering mean free path in strongly photonic media has been obtained.[26] To verify the design principle described above, we have infiltrated the Si nanowire sample with ethanol (refractive index $n = 1.36$). The total hemispherical reflectance before and after infiltration is shown in Figure 5a. A clear reduction of the reflectance is observed which is more pronounced toward higher photon energy. For an effective medium without scattering, the reflectivity would increase upon filling of the matrix with a higher-index medium, which clearly distinguishes specular reflectance from multiple scattering effects. At low energies, the change in reflectance is much lower which indeed can be attributed to the large contribution of

the specular reflections of the nanowires and the substrate (dashed line in Figure 5a).

We have also investigated longer Si nanowires of up to 30 μm in length. For these long wires, diffuse multiple scattering results in a large hemispherical reflectance over the whole energy range from 0.7−2.2 eV (thin line in Figure 5b). Infiltration with ethanol in this case results in an overall reduction of the reflectance by 16%, as shown by the thick line in Figure 5b. The observed suppression of the diffuse reflectance in Figure 5a,b corresponds well with calculations using eq 2 for an increase of the scattering mean free path by a factor 3.0 (red lines in Figure 5a,b). A stronger suppression of diffuse light scattering will be possible using filling with high-index materials such as ITO ($n \sim 1.95$), used as transparent conductor in solar cells. Embedding of the nanowires in high-refractive index media will however again result in an increase of the specular reflectance of the layer. Alternatively, suppression of light scattering can be achieved by reducing the diameter of the nanowires below 30 nm.[15] Such a reduction will pose challenges with respect to the electronic properties of the nanowires, such as full wire depletion. It may also be possible to utilize an entirely different regime of micrometer-sized pillars, where light can be trapped by multiple reflections at the surface texture.[27] Another exciting possibility for designing light scattering which we point out here is the use of anisotropic scattering for enhancement of the photon trapping efficiency inside the layer. The cylindrical geometry and good alignment of the nanowires provide an ideal material in which scattering should take place preferentially in the plane. Investigation of this effect will be a topic of future research.

In conclusion, we have demonstrated that the optical properties of nanowire layers relevant for solar cell applications are governed by strong multiple scattering of light. A new design principle is found for the efficiency of light absorpton in these layers, which involves the optimization of the ratio of nondiffuse absorption length to the diffuse scattering length l_a/l_t. We have successfully demonstrated strong suppression of the total reflectance losses for InP nanowires over a wide spectral region. For Si nanowires, the large l_a/l_t ratio results in considerable diffuse reflectance losses. Tailoring of the scattering strength of nanowire materials is possible by varying the nanowire diameter or using refractive index matching. For applications in solar-energy harvesting, where a maximum spectral irradiance occurs in the green spectral region, control and design of light scattering in nanowire-based devices will be crucial in maximizing their performance.

Acknowledgment. The authors thank G. Immink, M. T. Borgström, and T. van der Beek for their technical support. This work was supported by The Netherlands Foundation "Fundamenteel Onderzoek der Materie (FOM)" and the "Nederlandse Organisatie voor Wetenschappelijk Onderzoek (NWO)," and is part of an industrial partnership program between Philips and FOM.

References

(1) Huynh, W. U.; Dittmer, J. J.; Alivisatos, A. P. *Science* **2002**, *295*, 2425–2427.
(2) Law, M.; Greene, L. E.; Johnson, J. C.; Saykally, R.; Yang, P. *Nat. Mater.* **2005**, *4*, 455–459.
(3) Baxter, J. B.; Aydil, E. S. *Appl. Phys. Lett.* **2005**, *86*, 1–3, 053114.
(4) Tian, B.; Zheng, X.; Kempa, T. J.; Fang, Y.; Yu, N.; Yu, G.; Huang, J.; Lieber, C. M. *Nature* **2007**, *449*, 885–888.
(5) K, Peng.; Y, Xu.; Y, Wu.; Y, Yan.; S.-T., Lee.; J., Zhu. *Small* **2005**, *1*, 1062–1067.
(6) Tsakalakos, L.; Balch, J.; Fronheiser, J.; Korevaar, B. A.; Sulima, O.; Rand, J. *Appl. Phys. Lett.* **2007**, *91*, 1–3, 233117.
(7) Goodey, A. P.; Eichfeld, S. M.; Lew, K.-K.; Redwing, J. M.; Mallouk, T. E. *J. Am. Chem. Soc.* **2007**, *129*, 12344–12345.
(8) Kayes, B. M.; Lewis, N. S.; Atwater, H. A. *J. Appl. Phys.* **2005**, *97*, 21–11, 11430.
(9) Hu, L.; Chen, G. *Nano Lett.* **2007**, *7* (11), 3249–3252.
(10) Yang, Z.-P.; Ci, L.; Bur, J. A.; Lin, S.-Y.; Ajayan, P. M. *Nano Lett.* **2008**, *8*, 446–451.
(11) Chen, X.; Mao, S. S. *Chem. Rev.* **2007**, *107*, 2891–2959.
(12) Derkacs, D.; Lim, S. H.; Matheu, P.; Mar, W.; Yu, E. T. *Appl. Phys. Lett.* **2006**, *89*, 1–3, 093103.
(13) Pillai, S.; Catchpole, K. R.; Trupke, T.; Green, M. A. *J. Appl. Phys.* **2007**, *101*, 1–8, 093105.
(14) Muskens, O. L.; Borgström, M. T.; Bakkers, E. P. A. M.; Gómez Rivas, J. *Appl. Phys. Lett.* **2006**, *89*, 1–3, 233117.
(15) Muskens, O. L.; Diedenhofen, S. D.; Borgström, M. T.; Bakkers, E. P. A. M.; Gómez Rivas, J. *Adv. Funct. Mater.* **2008**, *18*, 1039–1046.
(16) Wagner, R. S.; Ellis, W. C. *Appl. Phys. Lett.* **1964**, *4*, 89–91.
(17) Xi, J.-Q.; Schubert, M. F.; Kim, J. K.; Schubert, E. F.; Chen, M.; Lin, S.-Y.; Liu, W.; Smart, J. A. *Nature Phot.* **2007**, *1*, 176–178.
(18) Bohren, C. F.; Huffman, D. R. *Absorption and scattering of light by small particles, 1st ed.*; Wiley-VCH: Weinheim, 1998.
(19) Aspnes, D. E.; Studa, A. A. *Phys. Rev. B* **1983**, *27*, 985–1009.
(20) Gómez Rivas, J.; Sprik, R.; Lagendijk, A.; Noordam, L. D.; Rella, C. W. *Phys. Rev. E* **2001**, *63*, 1–12, 046613.
(21) Van der Hulst, H. C. *Light scattering by small particles, 1st ed.*; Wiley: New York, 1957.
(22) Lagendijk, A.; Vreeker, R.; de Vries, P. *Phys. Lett. A* **1989**, *136*, 81–88.
(23) Zhu, J. X.; Pine, D. J.; Weitz, D. A. *Phys. Rev. A* **1991**, *44*, 3948–3959.
(24) (a) Ishimaru, A. *Wave propagation and scattering in random media*, Vols. I and II; Academic: New York, 1978. (b) Genack, A. Z. *Phys. Rev. Lett.* **1987**, *58*, 2043–2046.
(25) Wang, J.; Gudiksen, M. K.; Duan, X.; Cui, Y.; Lieber, C. M. *Science* **2001**, *293*, 1455–1457.
(26) Schuurmans, F. J. P.; Vanmaekelbergh, D.; van de Lagemaat, J.; Lagendijk, A. *Science* **1999**, *284*, 141–143.
(27) Wu, C.; Crouch, C. H.; Zhao, L.; Carey, J. E.; Younkin, R. J.; Levinson, J. A.; Mazur, E.; Farrel, R. M.; Gothoskar, P.; Karger, A. *Appl. Phys. Lett.* **2000**, *78*, 1850–1852.

NL0808076